# Immobilization of Zirconocene into Silica Prepared by Non-Hydrolytic Sol-Gel Method

*Adriano Fisch,*[1] *Cristiane F. Petry,*[2] *Dirce Pozebon,*[2] *Fernanda C. Stedile,*[2]
*Nilo S. M. Cardozo,*[1] *Argimiro R. Secchi,*[1] *João H. Z. dos Santos**[2]

**Summary:** Concomitant immobilization of zirconocene ($Cp_2ZrCl_2$) into a silica matrix was performed during the $SiO_2$ synthesis through non-hydrolytic sol-gel method. Two different routes, varying the $SiCl_4$:$Si(OEt)_4$ ratio were evaluated in terms of zirconocene content and catalyst activity in ethylene polymerization, using methylaluminoxane (MAO) as cocatalyst. The catalysts were characterized by Rutherford backscattering spectrometry, Fourier transform infrared spectroscopy, diffuse reflectance spectroscopy, scanning electron microscopy and X-ray dispersive spectroscopy. The zirconocene content laid between 0.60 and 1.02 wt.% Zr/$SiO_2$, depending upon the components ratio employed in the sol-gel synthesis. Catalyst grains presented of irregular shape (20–100 μm size) and zirconocene distribution was not uniform. Both routes led to supported catalysts active in ethylene polymerization. Catalyst activity was intermediate between that exhibited by the homogeneous and the grafted zirconocene on silica. Resulting polyethylenes presented narrow molecular weight distribution and molecular weight slightly higher than that observed in the case of polymer produced with the homogeneous system.

**Keywords:** polyethylene; polymerization; sol-gel; supported metallocene

## Introduction

Metallocene catalysts can polymerize α-olefins with high activity and excellent stereochemical control. Such catalysts made possible the industrial production of precisely controlled polymers such as linear low-density polyethylene, isotactic polypropylene, syndiotactic polypropylene, syndiotactic polystyrene, for instance. The key of the success resides in the fact that in such very active systems, the control of the coordination sphere around the metal center allows to define the polymer properties.[1] Nevertheless, the industrial application into the current plants, which are designed to run heterogeneous Ziegler-Natta catalysts, is only possible if such systems are supported on suitable carrier.

In order to generate heterogeneous metallocene systems, several methods have been proposed in the literature.[2] Silica has been largely the most employed support. Nevertheless, other supports have been investigated such as mobile crystalline materials (MCM), SBA-15, and zeolites, as well as organic supports such as polymers.[3–7] In the case of silica, grafting takes place through a surface reaction between the silanol groups and the ligand (usually chloro) of the metallocene. Grafted Zr content depends on the number and on the nature of the silanol groups, which, in turn, are determined by the previous thermal and chemical treatments of the support.[8] In other words, the potential immobilization

---

[1] Escola de Engenharia, Departamento de Engenharia Química – Universidade Federal do Rio Grande do Sul – r. Eng. Luiz Englert s/n – 90040-040 – Porto Alegre - Brazil
[2] Instituto de Química - Universidade Federal do Rio Grande do Sul- Av. Bento Gonçalves, 9500 - 91509-900 - Porto Alegre – Brazil
E-mail: jhzds@iq.ufrgs.br

sites on the surface limit the grafted metal content. Besides, the steric effect impinged by the grafted species and by the silica surface itself influences the nature and number of active sites.[9] In order to overcome such problems, some approaches have been proposed in the literature. For instance, chemical modifiers such as MAO,[3,10] TMA,[11] and organosilanes[12] have been proposed to generate more stable and spaced surface species, avoiding bimolecular deactivation reactions. Concerning the limited availability of silica silanol groups (dependent on the thermal treatment), methods based on the metallocene synthesis directly on the support have been investigated. For instance, silica-grafted $Ind_2ZrCl_2$ has been in situ synthesized after chlorinating with $SiCl_4$.[13] Hybrid silicas, bearing indenyl ligands were also employed for the preparation of supported zirconocenes.[14] In other words, different approaches for the immobilization of zirconocenes have been investigated in the literature, which differ on the catalyst activity and on the properties of the resulting polymers. Nevertheless, for the knowledge of the authors, concomitant immobilization of zirconocenes into silica matrix together the $SiO_2$ synthesis obtained by sol-gel method has not been already reported.

Sol-gel processes allow to obtain solid materials by gelation where the oxide network is created by progressive polycondensation reactions of molecular precursors in liquid medium, or as a process to form materials via a sol, gelation of the sol and finally removal of the solvent. According to Schubert and Hüsing, this method is considered as a soft chemical approach to the synthesis of amorphous oxide materials in comparison to the crystallization or precipitation methods.[15] However, typical routes present disadvantages associated with the use of water when the objective is immobilizing metallocene catalysts due to its chemical lability. Therefore, for zirconocene immobilization, a non-hydrolytic sol-gel route is necessary. In this route, a metal halide reacts with an alkoxysilane, catalyzed by a Lewis acid, forming the oxide. The structure of silica particles obtained by the sol-gel method is usually composed by aggregation of elementary, or primary, structures having 10–100 nm in order of magnitude.[16] Taking into account this, it hypothesized that the metallocence could be retained among the aggregates of primary structures within the silica matrix.

In order to evaluate this method for heterogeneization of metallocenes, the present work reports the results obtained on the immobilization of $Cp_2ZrCl_2$ within the silica matrix using a non-hydrolytic sol-gel process. The resulting supported systems were characterized by spectroscopic techniques and evaluated in ethylene polymerization, using MAO as cocatalyst.

## Materials and Methods

### Chemicals and Reagents

All the employed chemicals were analytical reagent grade and all experiments were performed under inert atmosphere (Argon) using the Schlenk technique. Silicon tetrachloride (Merck), tetraethylorthosilicate (TEOS, Merck) and triethylaluminium toluene solution (TEA; Akzo Nobel) were used without further purification. Cyclopentadienil zirconium dichloride ($Cp_2ZrCl_2$; Aldrich) was used as received. Toluene and n-hexane were purified by distillation on metallic sodium and benzofenone. Iron(III) chloride (95%; Merck) was dried by vacuum at room temperature for 2 h. Silica Grace 948 ($255\ m^2\ g^{-1}$) was activated under vacuum ($P < 10^{-4}$ mbar) for 16 h at 450 °C. The support was then cooled to room temperature under dynamic vacuum and stored under dried Argon. Sulphuric acid ($H_2SO_4$) and $1000\ mg\ L^{-1}$ Zr stock solution from Merck were used for Zr determination by means of ICP OES. Calibration solutions ranging from 5 to $20\ \mu g\ L^{-1}$ of Zr were prepared by serial dilution of the stock Zr solution in 10% v/v $H_2SO_4$ (prepared in deionized water – resistivity of $18.2\ M\Omega \cdot cm$).

## Metallocene Encapsulation

In order to define the adequate route to heterogenisation of the zirconocene by concomitant immobilization with the silica synthesis several studies were previously carried out based on the studies of Hay and Raval and Bourget *et al.* about the non-hydrolytic sol-gel.[17,18] However, modifications were done due to thermal liability of the metallocenes, for instance. Scheme 1 shows the routes evaluated in this study.

In route **A**, the zirconocene was added into the system after a previous reaction between TEOS (3.80 cm$^3$) and $SiCl_4$ (4 cm$^3$) in the presence of $FeCl_3$ (0.02 g), which is the Lewis acid. This reaction was accomplished at 110 °C in accordance with references 17 and 18. Afterwards, the system was cooled to 70 °C and the metallocene solution (0.3 g in 5ml of toluene) was added, and the reaction was carried out for 5 h.

In route **B**, the zirconocene (0.3 g) was added together with $FeCl_3$ (0.02 g) in the presence of a coordinationg solvent (THF, 20 cm$^3$). The reaction was carried out at 70 °C to avoid thermal degradation of the metallocene. The reaction was led for 5h.

In route **C**, the zirconocene was dissolved in toluene (1 cm$^3$), followed by the addition of the $FeCl_3$ (0.02 g), $SiCl_4$ and TEOS. The reaction was accomplished at 70 °C. After the gelation time has been reached (3 h), the resulting oxide was washed (20 × 2 cm$^3$) with a TEA n-hexane solution (ca. 0.5 wt.%) at room temperature in order to eliminate residual ethoxide groups.[14] The solid was further dried by vacuum for 12 h at room temperature. It was used two molar ratio $SiCl_4$:TEOS in order to study its effects on the performance of the catalyst: 1:1 (**C11**) and 2:1 (**C32**).

For comparative reasons, the corresponding grafted zirconocene was synthesized according to the protocol described in the literature.[8]

## Catalyst Characterization

### *Rutherford Backscattering Spectrometry (RBS)*

Zr loadings in catalysts were determined by Rutherford Backscattering Spectrometry (RBS) using He$^+$ beam of 2.0 MeV incident on homogeneous tablets of the compressed (12 MPa) powder of the catalyst systems. During analysis the base pressure in the chamber was kept in the $10^{-7}$ mbar range using membrane (to prevent oil contamination of the sample) and turbodrag molecular pump. The method is based on the determination of the number and the energy of the detected particles, which are elastically scattered in the Coulombic field of the atomic nuclei in the target. In this study, the Zr/Si atomic ratio was determined from the heights of the signals corresponding to each of the elements in the spectra and converted to wt.-% Zr/$SiO_2$. For an introduction to the method and applications of this technique the reader is referred elsewhere.[19]

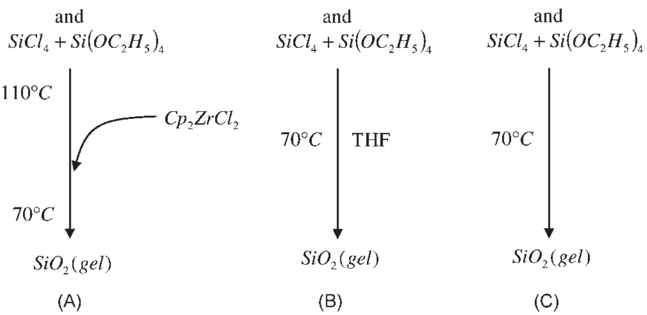

***Scheme 1.***

### *Inductively Coupled Plasma Optical Emission Spectroscopy*

An inductively coupled plasma optical emission (ICP OES) spectrometer from PerkinElmer (Optima™ 2000 DV) was used for Zr measurement in the catalyst leaching tests. A Scott spray chamber and a GemCone® nebulizer composed the sample introduction system. The leaching of the analyzed samples was added of $H_2SO_4$ (10%, v/v) and placed in Teflon® capped vessel. Then, the mixture was heated at 160 °C for 9 h in a heating block (Tecnal, Piracicaba, SP, Brazil). Samples and blanks were analyzed in triplicate.

### *Fourier-Transformed Infrared Spectroscopy (FT-IR)*

Infrared Spectroscopy measurements were carried out in a Shimadzu FTIR 8300 spectrophotometer coadding 32 scans at 4 $cm^{-1}$ resolution. Samples were analyzed in transmission mode as self-supported pellets.

### *Ultraviolet – Diffuse Reflectance Spectroscopy (UV-DRS)*

Diffusion reflectance in the UV-vis region was measured in a Varian Cary 100. Samples were prepared as self-supported pellets.

### *X-Ray Diffraction Spectroscopy (XRD)*

The XRD analyses were performed in a Rigaku (DMAX 2200) difractometer equipped with a Cu tube and secondary monochromator, theta-theta Ultima goniometer and scintillation (NaI (Tl)) detector. Samples were analyzed as powder at room temperature.

### *Scanning Electron Microscopy and X-Ray Energy-Dispersive Spectroscopy (SEM-EDX)*

Scanning Electron Microscopy (SEM) and X-Ray Energy Dispersive (EDX) were performed in a JSM 5800 (JEOL) microscope, operating between 10 and 20 kV. The samples were coated with thin layer of conductive carbon by sputtering technique.

### *Nitrogen Sorption Studies*

A Micrometeritics Gemini was used for nitrogen sorption studies. The samples were preheated at 70 °C for 8 h under vacuum before each measurement. The specific surface area was determined by the Brunauer-Emmett-Teller (BET) method at −196 °C, in the partial pressure range of $0.01 < P/P0 < 0.25$. The total pore volume was obtained from the $N_2$ desorption isotherm.

## Polymerization Reactions

Ethylene polymerization reactions were performed in 150 $cm^3$ of toluene in a 300 $cm^3$ Pyrex glass reactor connected to a constant temperature circulator and equipped with magnetic stirring and inlets for argon and the monomer. MAO was used as cocatalyst in the Al/Zr range from 1000 to 2000. For each experiment, a mass of catalyst system corresponding to $10^{-5}$ M of the metal was suspended in 5 $cm^3$ of toluene and transferred into the reactor under argon. The polymerizations were performed with 1.6 bar of absolute pressure of ethylene for 30 min. at 60 °C. Acidified (HCl) ethanol was used to quench the processes, and reaction products were separated by filtration, washed with distilled water, and finally dried under reduced pressure at 60 °C.

Catalyst leaching test was performed using a mass of catalyst corresponding to $10^{-6}$ mol of Zr which was suspended into 150 $cm^3$ of toluene with MAO ($Al/Zr = 2000$) under Argon. The system was stirred for 1 h at 60 °C and then filtered through a fritted disk. The filtered solution was transferred into the reactor under Argon. The polymerization reactions were carried out with 1.6 bar of ethylene pressure, at 60 °C for 30 min. Acidified (HCl) ethanol was used to quench the process. Also, ICP-OES was used for determining the Zr content in the eluated.

## Polymer Characterization

Polymers were characterized by melting point and crystallinity using a Perkin-Elmer DSC 4 differential scanning calorimeter. The instrument was calibrated with Indium and the measurements were performed using a heating rate of 10 °C $min^{-1}$ in the temperature range of 40–240 °C. The heating cycle was performed twice, but only the results of the second scan are reported, since the former is influenced by the mechanical and thermal history of the samples. Molar masses and molar mass distributions were investigated with a Waters 150C high-temperature GPC instrument, equipped with refraction index detector and three columns (Styragel® HT 3, HT 5 e HT 6E toluene). The columns were calibrated with standard polystyrenes of narrow molar mass distribution and with linear low-density polyethylenes and polypropylenes. TCB was used as solvent at a flow rate of 1 $cm^3 \cdot min^{-1}$. The analyses were performed at 140 °C using ca. 2 mg of mass samples, which was previously dissolved in 4 $cm^3$ of 1,2,4 -trichlorobenzene (TCB) in the oven at 180 °C for 1 h.

## Results and Discussion

### Catalyst Synthesis

In route **A** (Scheme 1), the metallocene was added into the medium after a short period of reaction between the TEOS and $SiCl_4$ in order to allow the formation of the primary structures of the silica matrix. After the addition of the metallocene solution, no gel could be observed after 5h of stirring time. Perhaps, the solvent, necessary to dissolve the zirconocene is interfering in the kinetic mechanism of sol formation retarding, or even preventing silica network crosslinking formation.

In route **B** (Scheme 1), the zirconocene was added together with $FeCl_3$ and coordinating solvent (THF) was used. In this route, the growth of primary structures occurred in the presence of the metallocene. The reaction was carried out at 70 °C during 5h, but the gelification did not occur during this time.

In route **C** (Scheme 1), the zirconocene was dissolved in a small volume of toluene (1 $cm^3$), followed by the addition of the $FeCl_3$, $SiCl_4$ and TEOS. In this route, for both molar ratios, the gelification has been reached around 4h. The resulting oxide was washed with a TEA n-hexane solution (ca. 0.5 wt.%) at room temperature in order to eliminate residual ethoxide groups.[14] Characterization of the catalysts obtained through route C was accomplished as follow.

### Catalyst Characterization

Table 1 shows the resulting immobilizing zirconium content within the catalysts obtained by route C.

In the routes **C11** and **C21**, it was used the ratio 1:1 (stoichiometric) and 2:1 of the $SiCl_4$:$Si(OC_2H_5)_4$, respectively. When excess of $SiCl_4$ was employed (**C21**), all the $Si(OC_2H_5)_4$ might be reacted and the generated mass of oxide matrix is higher than by stoichiometric route (**C11**) probably due to equilibrium displacement. Therefore, the route **C11** has exhibited higher contents of the zirconium in the catalyst that could be attributed to lower conversion (lower yield) of the reactants to oxide matrix. According to Table 1, the zirconium content is related to the $SiCl_4$:-$Si(OC_2H_5)_4$ ratio.

The catalysts were further characterized by complementary techniques. Figure 1 shows a typical IR spectrum of the immobilized catalysts.

Most of the assigned bands (see Table 2) refers to the oxide matrix.[20–22]

According to Figure 1, the presence of silica can be observed by the presence of a strong band centered at 1090 $cm^{-1}$, attributed to the Si–O–Si stretching, which was present in both catalysts. The band presented at 1174 $cm^{-1}$ can be assigned to Si–O–C stretching, probably due to residual ethoxide groups, confirmed also by the presence of C–H stretching at 3000–2900 $cm^{-1}$ region. Besides, surface species resulting from the treatment with TEA might also have generated Si–O–C species. The C–C

***Table 1.***
$Cp_2ZrCl_2$ immobilized into oxide matrices.

| Route | Encapsulated zirconocene (wt.% $Zr/SiO_2$) |
|---|---|
| C11 | 1.02 |
| C21 | 0.60 |

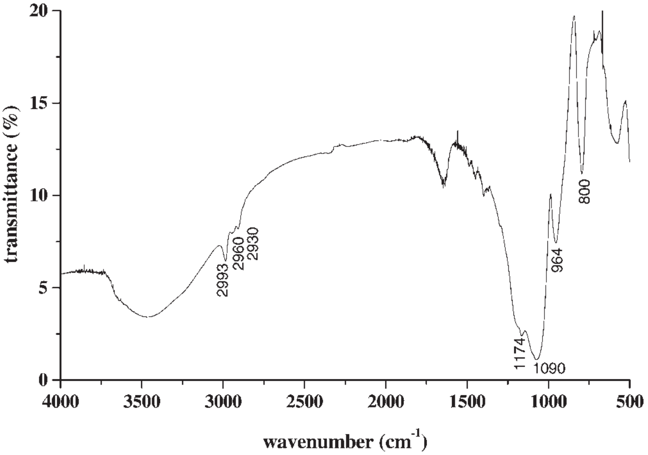

***Figure 1.***
FT-IR spectrum of immobilized zirconocene obtained by route C11.

stretching and C–H out-of-plane deformation of cyclopentadienyl rings might be overlaid by Si–O–Si and OH (geminal) on the all spectra. Therefore, confirmation of the presence of the zirconocene into silica matrix was not possible by FTIR measurement.

The catalysts were further analyzed by UV-DRS in order to try to detect the presence of the zirconocene species. Figure 2 shows the spectra of the encapsulated catalysts.

According to Figure 2, two bands are observed in the case of $Cp_2ZrCl_2$, at 320 and 370 nm, which could be assigned to ligand metal charge transfers (LMCT) Cl → Zr and Cp → Zr, respectively.[23] The band attributed to LMCT Cp → Zr was also observed in both routes C11 and C21. The transition LMCT Cl → Zr is less clear and might be reduced due to Cl reaction during the oxide matrix synthesis or during the washing step with TEA.

The morphology of the catalysts was obtained by SEM images. Figure 3 shows the catalyst grain micrographies obtained for the route C11. The grain has irregular shape and sizes, which were shown to be in the range of 20–100 μm. Similar micrographies were observed for route C21.

The catalysts were further analyzed by SEM-EDX. Figure 4 shows the microanalysis of the encapsulated catalyst obtained by route C21. Elemental analysis distribution shows only the presence of Si. The presence of Zr is not detected by the microanalysis probably due to the high detection limit for this compound (around 1%).

Catalyst analysis by XRD, as expected, has shown that the oxide matrix was amorphous for both systems, presenting a broad halo centered at 22°, which is assigned to $SiO_2$. The determination of the porosity or pore radii by nitrogen sorption demonstrated that the immobilized metallocenes have low surface area, ca. 10 $m^2/g$, probably due to pore collapse during the drying process.

***Table 2.***
Main assignments of the FTIR.[20–22]

| Assignments | cm$^{-1}$ |
|---|---|
| $Si–O–C_2H_5$ (stretching) | 1174 |
| C–C (stretching) | 1155 |
| Si–O–Si, infinite chain (stretching) | 1090 |
| Si–O (angular deformation) | 964 |
| O–H, single (stretching) | 850 |
| C–H (out-of-plane deformation) | 830–701 |
| OH, geminal (stretching) | 800 |

## Catalyst Evaluation

The immobilized zirconocenes C11 and C21 were evaluated in ethylene polymerization having MAO as cocatalyst. Table 3

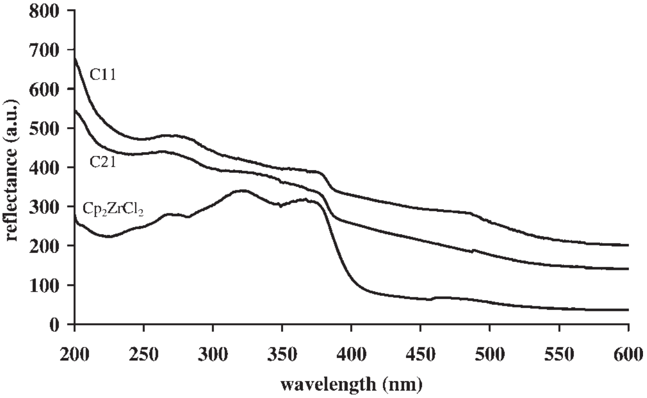

***Figure 2.***
UV-DRS spectrum of the immobilized catalysts.

shows the results in catalyst activity. For comparative reasons, data from the homogeneous catalyst and from that grafted on silica were also included.

As shown in Table 3, the catalysts C11 and C21 were active in ethylene polymerization. The highest activity was observed for the catalyst obtained by route C11 at Al/Zr = 2000. Nevertheless, the catalyst did not show suitable activity at lower Al/Zr ratios, which could be attributed to access hampering of the cocatalyst or to the deactivation after fragmentation. Further investigation is necessary to elucidate this question.

It is worth noting that the supported catalyst obtained by grafting on silica presented lower activity than the immobilized metallocene C11 and C12. In comparison to the homogeneous system, such behavior is expected since the silica surface plays the role of huge ligand hindering the access to the monomer. The immobilized systems present intermediate catalyst activity, suggesting that the homogeneous nature of the zirconocene might have been preserved. Nevertheless, in this case, the access of the monomer to catalyst centers is also hampered being probably responsible for the reduction in catalyst activity in

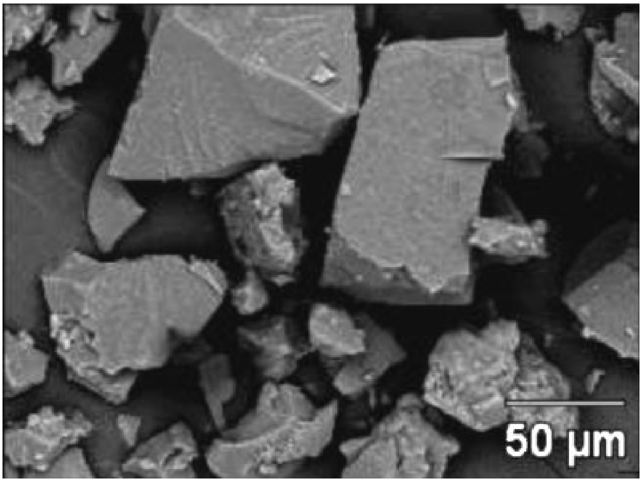

***Figure 3.***
SEM micrographics of catalyst C11.

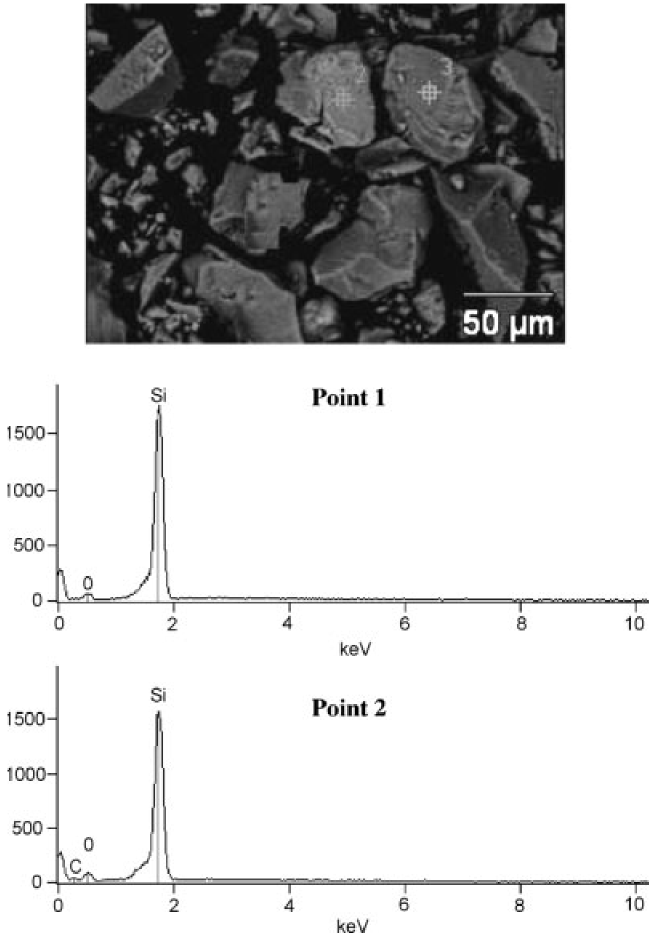

***Figure 4.***
Elemental distribution in catalyst C21, measured by SEM-EDX.

comparison to the homogeneous one. Comparing the immobilized to the grafted system, the former, as already mentioned, presents higher catalyst activity. Silica grafted systems are know to be much less active. In addition to the steric effect played by the support itself, it is believed that only roughly ca. 1.0% of the total grafted species

***Table 3.***
Catalyst activity and polymer characteristics.

| Catalyst | Al/Zr | Activity ($kg_{pol} \cdot mol_{Zr}^{-1}$) | $T_m$ (°C) | $\chi$ (%) | $M_w$ ($kg \cdot mol^{-1}$) | $M_w/M_n$ |
|---|---|---|---|---|---|---|
| C11 (1.02 wt.% Zr/$SiO_2$) | 2000 | 1900 | 135 | 70 | 153 | 2.1 |
| | 1500 | 220 | 134 | 51 | 133 | 2.6 |
| | 1000 | 80 | 133 | 46 | 130 | 2.5 |
| C21 (0.60 wt.% Zr/$SiO_2$) | 2000 | 1400 | 133 | 51 | 230 | 2.0 |
| | 1500 | 135 | 132 | 56 | 130 | 3.2 |
| | 1000 | traces | – | – | – | – |
| $Cp_2ZrCl_2$ | 2000 | 3000 | 133 | – | 100 | 2.2 |
| | 1500 | 2750 | 133 | 66 | 120 | 2.3 |
| $Cp_2ZrCl_2/SiO_2$ (0.4 wt.% Zr/$SiO_2$) | 2000 | 1300 | 136 | – | 90 | 2.8 |

is indeed active.[24] Thus, since in the present immobilization process, no reaction between silanol groups and zirconocene ligands are involved (as in the case of grafting), this process is not responsible for the lower activity. In this case, the monomer access to zirconocene molecules inside the silica support might be the major limiting factor influencing catalyst activity. Especially since very low specific surface areas were determined by the BET method, suggesting the presence of a silica matrix with very low porosity.

The stability of the immobilized catalysts in terms of leaching from MAO cocatalyst was evaluated through measuring Zr in the eluted fraction. According to ICP-OES analysis, Zr metal content in solution was shown to be about 10 $\mu$g L$^{-1}$ for both catalysts. Therefore, leaching process during polymerization was considered very negligible.

## Polymer Characterization

The resulting polyethylenes were characterized through DSC and GPC (Table 3). Melting temperature ($T_m$) and the degree of crystallinity ($\chi$) ranged from 44 to 70%, being these values expected for high-density polyethylene. It is curious that the molecular weight observed for the polymers obtained with the immobilized zirconocenes is slightly higher than that produced with the homogeneous one. It seems that the silica matrix might impinge some effect during the polymerization process hindering, for instance, termination reactions or affording a higher stability of the catalyst center during polymer chain growing steps. Further studies are necessary to elucidate such possibilities.

The morphology of the nascent polymers (polymers obtained in the early stages of the polymerization) was evaluated through the SEM (Figure 5).

It could be noticed that the polymer obtained with immobilized zirconocene have more similar morphology with homogeneous catalyst than with the supported on commercial silica.

## Final Remarks

Concomitant zirconocene immobilization into a silica matrix during the synthesis of $SiO_2$ by non-hydrolytic sol-gel method was shown to be a potential strategy for developing heterogeneous metallocene catalysts. This preliminary study has shown

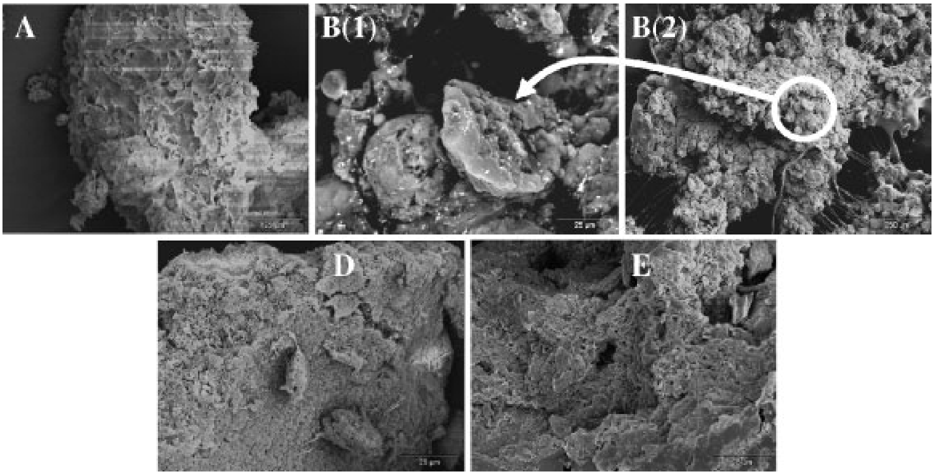

*Figure 5.*
SEM micrographics for nascent polymers. Homogeneous polymerization of zirconocene (A, magnification 1000×), supported zirconocene on silica 948 (B(1) and B(2), magnification 1000× and 100×, respectively), immobilized catalyst C21 (C, magnification 1000×), immobilized catalyst C11 (D, magnification 1000×).

that the ratio of the matrix components influences on the immobilized zirconium content as well as on the catalyst activity in ethylene polymerization. In spite of the fact that the nature of the catalyst species might be closer to the homogeneous ones, the environment might somehow influence on the polymerization process, since polyethylenes with higher molecular weight were obtained. The heterogeneous distribution of zirconium in the grain and the very low catalyst specific surface area are drawbacks, which have to be overcome. Nevertheless this heterogeneisation route seems to allow to avoid some inconvenient usually observed in the case of zirconocene grafting, such as catalyst leaching or very low grafted content, which, in turn, depends on the availability of surface silanol groups and on the steric effect played by the coordination sphere of the metallocenes.

*Acknowledgements:* This project was partially supported by CNPq.

[1] See, for example: [1a] W. Kaminsky, "*Metalorganic Catalysts for Synthesis and Polymerization: Recent Results by Ziegler-Natta and Metallocene Investigations*", Springer-Verlag, Berlin, **1999**;

[1b] G. G. Hlakty, in: "*Metallocene-Based Polyolefins*", J. Scheirs, W. Kaminsky, Eds., John Wiley, West Sussex, **2000**;

[1c] H. Alt, A. Köppl, *Chem. Rev.* **2000**, *100*, 1205.

[2] J. R. Severn, J. C. Chadwick, R. Duchateau, N. Friederichs, *Chem. Rev.* **2005**, *105*, 4073.

[3] C. Liu, T. Tang, B. Huang, *J. Catal.* **2004**, *221*, 162.

[4] X. Dong, L. Wang, G. Jian, Z. Zhao, T. Sun, H. Yu, W. Wang, *J. Mol. Catal. A: Chem.* **2005**, *240*, 239.

[5] M. F. V. Marques, S. C. Moreira, *J. Mol. Catal. A: Chem.* **2003**, *192*, 93.

[6] Y. S. Ko, S. I. Woo, *Eur. Polym. J.* **2003**, *39*, 1553.

[7] L. Wu, J.-M. Zhou, D. T. Lynch, S. E. Wanke, *Appl. Catal.* **2005**, *293*, 180.

[8] J. H. Z. dos Santos, S. Dorneles, F. C. Stedile, J. Dupont, M. C. Forte, I. J. R. Baumvol, *Macromol. Chem. Phys.* **1997**, *198*, 3529.

[9] J. H. Z. dos Santos, C. Krug, M. B. da Rosa, F. C. Stedile, J. Dupont, M. C. Forte, *J. Mol. Catal. A: Chem.* **1999**, *139*, 199.

[10] M. C. Haag, J. Dupont, F. C. Stedile, J. H. Z. dos Santos, *J. Mol. Cat. A: Chem.* **2003**, *197*, 223.

[11] F. G. Costa, E. A. Braga, S. T. Brandão, A. F. Espeleta, Z. N. da Rocha, L. M. T. Simplício, E. A. Sales, *Appl. Catal. A: Gen.* **2005**, *290*, 221.

[12] C. Alonso, A. Antiñolo, F. Carrillo-Hermosilla, P. Carrión, A. Otero, J. Sancho, E. Villaseñor, *J. Mol. Cat. A: Chem.* **2004**, *220*, 285.

[13] K. Soga, H. J. Kim, T. Shiono, *Macromol. Chem. Phys.* **1994**, *195*, 3347.

[14] J. H. Z. Dos Santos, H. T. Ban, T. Teranishi, T. Uozumi, T. Sano, T. Soga, *Appl. Catal. A: Gen.* **2001**, *220*, 287.

[15] U. Schubert, N. Hüsing, "*Synthesis of Inorganic Materials*", 2nd ed., Ed. Wiley, Weinheim, **2005**.

[16] K-I. Kuramada, H. Nakabayashi, T. Murataki, M. Tanigaki, *Colloids Surf. A: Physicochem. Eng. Asp.* **1998**, *139*, 163.

[17] J. N. Hay, H. M. Haval, *J. Sol-Gel Sci. Technol.* **1998**, *13*, 109.

[18] L. Bourget, R. J. P. Corriu, D. Leclereq, P. H. Mutin, A. Vioux, *J. Non-Cryst. Solids* **1998**, *242*, 81.

[19] F. C. Stedile, J. H. Z. dos Santos, *Nucl. Inst. Meth. Phys. Res. B* **1998**, *136–138*, 1259.

[20] E. F. Vansant, P. Van Der Voort, K. C. Vrancken, "*Characterization and Chemical Modification of the Silica Surface*", Elsevier Science, Amsterdam, **1995**.

[21] N. B. Colthup, "*Introduction to Infrared and Raman Spectroscopy*", 3rd ed.,Academic, San Diego, **c1990**.

[22] K. Nakamoto, "*Infrared and Raman Spectra of Inorganic and Coordination Compounds*", 5th ed., John Wiley, New York, **1997**.

[23] F. G. Costa, E. A. Braga, S. T. Brandão, A. de F. Espeleta, Z. N. da Rocha, L. M. T. Simplício, E. A. Sales, *Appl. Catal. A: Gen.* **2005**, *290*, 221.

[24] A. Muñoz-Escalona, G. Hidalgo, P. Lafuente, M. F. Martinez-Nuñez, L. Méndez, W. Michiels, B. Peña, J. Sancho, "Proceeding of 5th International Congress on Metallocene Polymers", Metallocene Europe 98, March, Düsseldorf, Germany, p. 73.